LIM Kinase, a Newly Identified Regulator of Presynaptic Remodeling by Rod Photoreceptors After Injury

Weiwei Wang and Ellen Townes-Anderson

Department of Pharmacology, Physiology and Neuroscience, Graduate School of Biomedical Sciences, Rutgers, The State University of New Jersey, Newark, New Jersey, United States

Correspondence: Ellen Townes-Anderson, Department of Pharmacology, Physiology and Neuroscience, New Jersey Medical School, Rutgers Biomedical and Health Sciences, 185 S. Orange Avenue, Newark, NJ 07103, USA; andersel@njms.rutgers.edu.

Submitted: May 15, 2015
Accepted: November 5, 2015

Citation: Wang W, Townes-Anderson E. LIM kinase, a newly identified regulator of presynaptic remodeling by rod photoreceptors after injury. *Invest Ophthalmol Vis Sci*. 2015;56:7847–7858. DOI:10.1167/iovs.15-17278

Purpose. Rod photoreceptors retract their axon terminals and develop neuritic sprouts in response to retinal detachment and reattachment, respectively. This study examines the role of LIM kinase (LIMK), a component of RhoA and Rac pathways, in the presynaptic structural remodeling of rod photoreceptors.

Methods. Phosphorylated LIMK (p-LIMK), the active form of LIMK, was examined in salamander retina with Western blot and confocal microscopy. Axon length within the first 7 hours and process growth after 3 days of culture were assessed in isolated rod photoreceptors treated with inhibitors of upstream regulators ROCK and p21-activated kinase (Pak) (Y27632 and IPA-3) and a direct LIMK inhibitor (BMS-5). Porcine retinal explants were also treated with BMS-5 and analyzed 24 hours after detachment. Because Ca^{2+} influx contributes to axonal retraction, L-type channels were blocked in some experiments with nicardipine.

Results. Phosphorylated LIMK is present in rod terminals during retraction and in newly formed processes. Axonal retraction over 7 hours was significantly reduced by inhibition of LIMK or its regulators, ROCK and Pak. Process growth was reduced by LIMK or Pak inhibition especially at the basal (axon-bearing) region of the rod cells. Combining Ca^{2+} channel and LIMK inhibition had no additional effect on retraction but did further inhibit sprouting after 3 days. In detached porcine retina, LIMK inhibition reduced rod axonal retraction and improved retinal morphology.

Conclusions. Thus structural remodeling, in the form of either axonal retraction or neuritic growth, requires LIMK activity. LIM kinase inhibition may have therapeutic potential for reducing pathologic rod terminal plasticity after retinal injury.

Keywords: LIM kinase, axon retraction, retinal detachment, rod photoreceptors, Rho signaling

Photoreceptors demonstrate presynaptic structural remodeling in response to injury or disease. After retinal detachment, rod cells retract their axons and terminals from the outer plexiform layer (OPL), whereas cone cells respond by rounding their synaptic terminal.[1,2] In contrast, after retinal reattachment or during retinal disease, rod photoreceptors sprout neuritic processes.[3–8] Both axonal/terminal retraction and neuritic sprouting presumably disrupt the normal connectivity between photoreceptors and second-order neurons, and thus are potentially disruptive for vision. Here we focus on rod photoreceptor axonal retraction in response to the injury of retinal detachment.

Retinal detachment occurs with severe myopia, advancing age, complication from cataract surgery, or after trauma from high-impact or high-speed activities.[9–14] To prevent potential visual loss after detachment due to disrupted circuitry, it is necessary to understand the mechanisms behind the reactive structural changes by photoreceptors. RhoA-Rho kinase (ROCK) activity[15,16] and Ca^{2+} influx[17,18] have been reported to play a role in regulating axonal retraction by rod photoreceptors in both isolated tiger salamander rod cells and detached porcine retinas. This study expands these findings by examining (1) the role of ROCK's downstream effector, LIM kinase (LIMK)[19–21]; (2) the role of p21-activated kinase (Pak), like ROCK, an upstream regulator of LIMK[21–24]; and (3) the relationship between Ca^{2+} influx and ROCK or LIMK in rod cell injury.

LIM kinase regulates actin cytoskeletal dynamics, through cofilin, in various species and tissues.[25–28] Since rod axonal and neuritic plasticity requires morphologic change, actin filament rearrangement is presumably necessary. Thus LIMK activity is very likely to be involved in the response of photoreceptors to injury. However, involvement of LIMK does not preclude a role for actomyosin contraction, which has been suggested to coordinate with increased actin dynamics in complex physiological activities, such as axon guidance[29–31] and cell migration.[32–34] ROCK and Ca^{2+} influx, previously demonstrated to be necessary for axonal retraction, promote actomyosin contraction through regulating myosin light chain (MLC) and myosin light chain phosphatase (MLCP), and myosin light chain kinase (MLCK), respectively.[19,20,35–37] We postulate, therefore, that both actin filament turnover and actomyosin contraction contribute to rod cell axonal retraction (Fig. 1).

LIM kinase may also play a role in the photoreceptor response to injury in the form of neuritic process outgrowth.[5,7,38] LIM kinase is well known to function in regulating actin polymerization in cooperation with the pathways that promote nucleation and extension of new actin filament

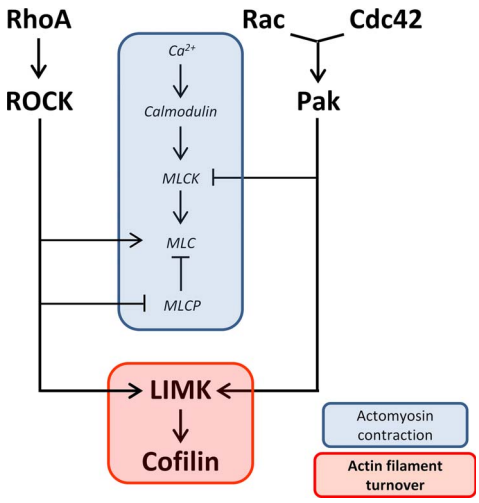

Figure 1. Diagram of proposed pathways involved in rod cell axonal and neuritic plasticity. Two activities, actomyosin contraction and actin filament turnover, are suggested to contribute to plasticity in the axon and axon terminal after injury. Both RhoA-ROCK and Cdc42/Rac-Pak pathways converge on LIMK, which promotes actin filament turnover through regulation of cofilin. However, while RhoA-ROCK promotes actomyosin contraction through activating MLC and inhibiting MLCP, Cdc42/Rac-PAK inhibits it through inhibiting MLCK. Ca^{2+}-calmodulin promotes actomyosin contraction through activating MLCK. RhoA, Rac, and Cdc42 are Rho GTPases; ROCK, Rho kinase; Pak, p21-activated kinase; LIMK, LIM kinase; MLC, myosin light chain; MLCP, myosin light chain phosphatase; MLCK, myosin light chain kinase.

branches.[39–41] Our study therefore also investigates the effect of LIMK inhibition on process outgrowth and explores the possibility that using inhibition of a single kinase, LIMK, can reduce both forms of structural plasticity, axonal retraction and neuritic sprouting.

Here we demonstrate the effectiveness of LIMK antagonism in stabilizing the structure of mature rod terminals of isolated salamander rod cells. We confirm the effect of LIMK inhibition on preventing axonal/synaptic retraction in the detached porcine retina. Pig eyes are a good model for retinal injury as porcine retina resembles human retina structurally and physiologically.[42–46] Finally, we demonstrate that LIMK, in conjunction with Ca^{2+}, also plays a role in neuritic sprouting. Thus, axonal retraction and neuritic sprouting appear to be linked by a common pathway.

Methods

Animals

Adult, aquatic-phase tiger salamanders (*Ambystoma tigrinum*, 18–23 cm in length) were used to obtain retinal tissue and cells. Salamanders were maintained at 5°C on a 12-hour light/12-hour dark cycle for 1 week before use. Porcine eyes from Yorkshire pigs (6 months old, weighing 65–80 kg) were obtained from a local slaughterhouse (Animal Parts, Scotch Plains, NJ, USA). All protocols were approved by the Institutional Animal Care and Use Committee (IACUC) at Rutgers, the State University of New Jersey, New Jersey Medical School and were in strict compliance with the ARVO Statement for the Use of Animals in Ophthalmic and Vision Research. A total of 52 tiger salamanders and 3 pigs were used in this study.

Pharmacologic Reagents and Antibodies

The direct LIMK inhibitor BMS-5 (SYN-1024; Synkinase, San Diego, CA, USA), Y27632 (C3912; Sigma-Aldrich Corp., St. Louis, MO, USA), IPA-3 (3622; Tocris, Bristol, UK), and nicardipine (N7510; Sigma-Aldrich Corp.) were dissolved in dimethyl sulfoxide (DMSO) before they were added to the culture medium. For cells and retinal explants, the final DMSO concentration was 0.5%.

The primary antibodies used were rabbit polyclonal anti-LIMK1 (No. 3842; Cell Signaling Technology, Danvers, MA, USA), rabbit polyclonal anti–phospho-LIMK1 (Thr508)/LIMK2 (Thr505) (No. 3841; Cell Signaling Technology), mouse monoclonal anti–glyceraldehyde-3-phosphate dehydrogenase (GAPDH, 1D4; sc-59540; Santa Cruz, Dallas, TX, USA), mouse monoclonal anti-synaptic vesicle protein 2 (SV2; Developmental Studies Hybridoma Bank, Iowa City, IA, USA), and mouse monoclonal anti-rhodopsin (4D2; MABN15; Millipore, Billerica, MA, USA). The secondary antibodies used were peroxidase-conjugated goat anti-rabbit IgG (111-035-045; Jackson ImmunoResearch, West Grove, PA, USA), peroxidase-conjugated goat anti-mouse IgG + IgM (115-035-068; Jackson ImmunoResearch), Alexa Fluor 488 donkey anti-rabbit IgG (A21206; Life Technologies, Carlsbad, CA, USA), and Alexa Fluor 647 goat anti-mouse IgG (A21236; Life Technologies).

Cell and Tissue Culture

Rod photoreceptors were obtained from salamander retinal dissociation as previously described.[47–49] Salamanders were decapitated, pithed, and enucleated. Retinas were digested in Ringer solution containing 14 U/mL papain (10108014001; Roche Life Science, Indianapolis, IN, USA) with agitation for 45 minutes. After rinsing and trituration, the cell suspension was plated onto glass coverslips coated with Sal-1 antibody (provided by Peter MacLeish, Morehouse School of Medicine, Atlanta, GA, USA) in 35-mm culture dishes as previously described.[50] Cultures were maintained in a dark, humidified incubator at 10°C in serum-free medium containing 108 mM NaCl, 2.5 mM KCl, 2 mM HEPES, 1 mM $NaHCO_3$, 1.8 mM $CaCl_2$, 0.5 mM NaH_2PO_4, 1 mM $NaHCO_3$, 24 mM glucose, 0.5 mM $MgCl_2$, 1 mM Na pyruvate, 7% medium 199, 1× minimum essential (MEM) vitamin mix, 0.1× MEM essential amino acids, 0.1× MEM nonessential amino acids, 2 mM glutamine, 2 μg/mL bovine insulin, 1 μg/mL transferrin, 5 mM taurine, 0.8 μg/mL thyroxin, 10 μg/mL gentamicin, and 1 mg/mL bovine serum albumin (pH 7.7). A total of 233 cell cultures from 46 tiger salamanders was examined (3403 rod photoreceptors in total, 10 to 15 cells per dish for axonal retraction and immunochemistry, 30 cells per dish for growth analysis). The numbers for each experiment are noted in the figure legends.

For salamander and porcine retinal explants, the anterior segment and vitreous body were removed from the eye. Whole salamander retinas were dissected free from retinal pigment epithelium (RPE) and incubated in the same conditions as cell cultures (described above). Porcine retinal explants were produced with a 7-mm-diameter trephine; for retinal detachment, the inner limiting membrane of the retina was overlaid by filter paper and the neural retina was gently teased away from the underlying RPE, choroid, and sclera, leaving the photoreceptor layer exposed. Because previous studies demonstrated quantitatively similar amounts of rod cell axonal retraction 24 hours after retinal detachment regardless of retinal region,[51] both the superior and inferior retina were used. Specimens were incubated in 12-well dishes in Neurobasal Medium (21103-049; Life Technologies) supplemented with B-27 (17504-044; Life Technologies) and 1.37 mM glutamine at 37°C. Medium was aerated with a humidified

Investigative Ophthalmology & Visual Science

mixture of 5% CO_2/95% O_2 for 24 hours after detachment. Twelve salamander retinal explants from six tiger salamanders and six porcine retinal explants from three pigs were cultured. Numbers for specific experiments are noted below and in the figure legends.

Measurement of Axonal Retraction in Isolated Cells

To examine axonal retraction, a Zeiss inverted light microscope (Axiovert S100TV; Carl Zeiss, Oberkochen, Germany), equipped with a motorized stage (Assy Stage 25; Cell Robotics, Inc., Albuquerque, NM, USA) and a 40×, 0.75 NA (numerical aperture) objective, was used to view retinal cultures. Rod photoreceptors were identified by morphology (cell shape and presence of an ellipsoid and axon terminal). Cells were selected by viewing the culture at an arbitrary location and then systematically scanning in rows. Rod cells with axon terminals (20–23 per dish) were selected by bright-field microscopy within the first hour after cell plating. At 7 hours, the same cells were located again. Their images were captured with a charge-coupled device camera (XC 75CE; Sony, Tokyo, Japan).

Axon length was measured with National Institutes of Health ImageJ 1.48 (http://imagej.nih.gov/ij/; provided in the public domain by the National Institutes of Health, Bethesda, MD, USA). Reduction in length, indicating retraction, was the difference between the axonal lengths at the first (L1) and seventh (L7) hour of the same cell. The percent decrease in length was calculated with the following formula: $(L1 - L7) \div L1 \times 100\%$.

Western Blotting

After a 2-hour incubation, detached salamander retinal explants were homogenized and lysed in ice-cold radioimmunorecipitation assay (RIPA) buffer (20-188; Millipore) supplemented with Complete Protease Inhibitor cocktail (04693116001; Roche Life Science), 1 mM Na_3VO_4, and 10 mM NaF. The lysate was clarified with centrifugation, 21,130*g* for 10 minutes at 4°C (5424; Eppendorf, Hauppauge, NY, USA). Protein concentrations were determined with the Bradford protein assay (500-0001; Bio-Rad, Hercules, CA, USA). Total lysate was boiled for 5 minutes in 2× Laemmli sample buffer (161-0737; Bio-Rad), and loaded onto a 12% Mini-Protean TGX SDS-PAGE Gel (456-1041; Bio-Rad). Equal amounts of lysate were loaded into each lane of the same gel; depending on the gel, the loaded lysate ranged from 6 to 15 μg protein. To confirm the detection of phosphorylated LIMK (p-LIMK), blots were incubated with 1 mL 5% BSA blocking buffer in the presence or absence of 1200 units of Lambda Protein Phosphatase (P0753S; NEB, Ipswich, MA, USA). Blots were probed with appropriate primary and peroxidase-conjugated secondary antibodies. SuperSignal West Femto Substrate (34094; Thermo Scientific, Somerset, NJ, USA) or SuperSignal West Dura Substrate (34077; Thermo Scientific) was used for detection. GAPDH was used as a loading control; blots were also subject to a Ponceau-S total protein stain (K793; AMRESCO, Solon, OH, USA).

Fluorescence Immunocytochemistry and Immunohistochemistry

Porcine retinas and salamander photoreceptor cell cultures were fixed with 4% paraformaldehyde in 0.1 M sodium phosphate buffer (PBS, pH 7.4) overnight at 4°C. Retinal explants were then embedded in 30% sucrose overnight at 4°C, frozen in optimal cutting temperature compound (No. 4583; Sakura, Torrance, CA, USA), and sectioned at 40 μm. Sections and cell cultures were immunolabeled with appropriate primary antibodies and fluorescent secondary antibodies. All specimens for each experiment were processed together. Control sections and cultures were processed simultaneously without primary antibodies. Specimens were mounted with ProLong Gold Antifade Mountant (P36930; Life Technologies) and sealed for further examination. For both retinal explants and rod photoreceptors, 1-μm optical sections were obtained with a laser scanning confocal microscope (LSM510; Carl Zeiss) equipped with argon and helium/neon lasers, a 40×, 1.2 NA water immersion objective, and a 63×, 1.4 NA oil immersion objective. Laser power, scan rate, objective, aperture, and exposure time were unchanged throughout each experiment for all specimens. Enhancements in brightness and contrast were performed with ImageJ (version 1.46r) only for presentation purposes.

Analysis of Process Growth

Rod photoreceptors in 3-day cultures were identified by rod opsin immunolabeling. Cells were selected for analysis by viewing the culture at an arbitrary location and then systematically scanning in rows. Every isolated rod photoreceptor encountered was digitally captured until 20 to 30 cells per dish were imaged. Process growth was examined by measuring the length of the longest process for each cell. In addition, the length of the longest process at the basal (nuclear) and the apical (ellipsoidal) pole of the cell was measured.

Measurement of Axonal Retraction in Retinal Sections

Porcine retinal sections were immunolabeled for SV2 and examined with confocal microscopy as described above. The immunolabel was analyzed (ImageJ 1.46r) by measuring the area of fluorescent signal within the outer nuclear layer (ONL) and reported as labeled area per 100 μm of retinal length. Data were collected from a total of 14 porcine retinal cryosections (6 porcine retinal explants from 3 animals, two or three cryosections per retinal explant); three or four different areas per cryosection were examined (see legend of Fig. 9).

Statistics

Data were analyzed with either Student's *t*-test or 1-way analysis of variance with Tukey's post hoc test for all pair-wise multiple comparisons (GraphPad Prism 5; GraphPad Software, La Jolla, CA, USA) and expressed as mean ± SEM. Significance was considered to be achieved at $P < 0.05$.

Results

Active LIMK Localizes in the Axon Terminal and Varicosities of Isolated Rod Photoreceptors

To study the activity of LIMK in rod cell presynaptic remodeling, we examined intact salamander retina and single, isolated rod photoreceptors for the presence of active LIMK, p-LIMK, with Western blot and immunocytochemistry, respectively.

Previous data in porcine retina indicated that the active form of RhoA, an upstream regulator of LIMK, is present soon after retinal detachment.[16] Here we detached salamander retina and incubated it for 2 hours to examine for LIMK in Western blot. Antibodies for both total-LIMK (t-LIMK) and p-

Investigative Ophthalmology & Visual Science

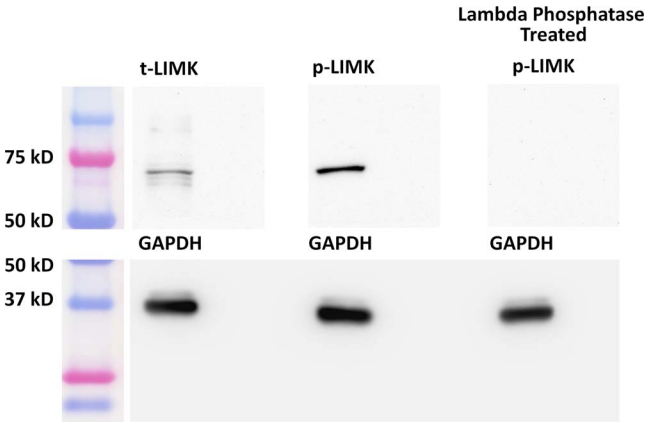

Figure 2. Active LIMK is present in salamander retina 2 hours after detachment. Antibodies against total-LIMK (t-LIMK, *upper left lane*) and phosphorylated LIMK (p-LIMK, *upper middle lane*) labeled a 72-kDa band. Lambda phosphatase–treated blot showed no band (*upper right lane*). GAPDH, from the same SDS-PAGE gel, served as an internal loading control (*lower lanes*). $n = 3$ animals, 6 retinal explants.

LIMK (Fig. 2, left and center lane, respectively) detected antigens at the appropriate molecular weight.[52] Lambda Phosphatase treatment to reduce p-LIMK eliminated all labeling (Fig. 2, right lane), confirming the detection of p-LIMK in detached retina.

Immunohistochemistry was then conducted to examine the distribution of t-LIMK and p-LIMK. Confocal microscopy revealed that t-LIMK is distributed throughout all retinal layers, including the ONL and OPL, where the photoreceptor somas and synaptic terminals reside, respectively (Fig. 3, right column). Phosphorylated LIMK is present both diffusely and in large spots throughout the normal, undetached retina; however, there is an apparent increase of p-LIMK 2 hours after detachment (Fig. 3, first and second columns). Comparisons were made within the same animal: One eye provided the normal retinal explant, and the other eye provided the detached retinal explant, which was incubated for 2 hours. The increase in p-LIMK label suggests that retinal detachment correlates with an increase in LIMK activity.

Next, we examined the localization of p-LIMK in isolated rod cells. To be consistent with previous studies,[15,16] we chose cells without an outer segment but with an axon terminal. Although rod opsin labeling predominantly localizes in the outer segments of rod photoreceptors in the intact retina, studies have shown that after retinal detachment and dissociation, rod opsin redistributes and is present throughout the entire plasma membrane of rod cells.[53] Here we used rod opsin labeling to confirm the identification of rod cells. Axon terminals retract over a 24-hour period in culture[18]; new processes appear at around 24 hours and develop presynaptic varicosities after several days in vitro.[48]

Enriched p-LIMK staining consistently appeared in the axon terminals of rod cells in 2-hour and 1-day cultures if the terminals had not yet completely retracted (Figs. 4Aa, 4Ab). In addition, varicosities in neuritic processes, which emerged from the basal (nuclear) pole and leading edge of lamellipodia (Fig. 4Ac) after 3 days in culture, also had strong p-LIMK labeling. Finally, labeling was present in the inner segment identified by the presence of the ellipsoid (an accumulation of mitochondria), of rod cells in 2-hour, 1-day, and 3-day cultures (Fig. 4A). There was little nonspecific labeling in controls (Fig. 4B).

Confocal microscopy at high magnification suggested that p-LIMK localization was cytosolic: The cell membrane was marked by opsin immunolabel, whereas the adjacent cytosol demonstrated p-LIMK labeling (Figs. 4Aa–4c). In some optical sections, overlap of the opsin and p-LIMK label was apparent. However, in these cases, the plane of the section through the plasma membrane was oblique. Thus, immunocytochemistry indicated the presence of active LIMK in rod axon terminals both while axons retract and later when outgrowth occurs.

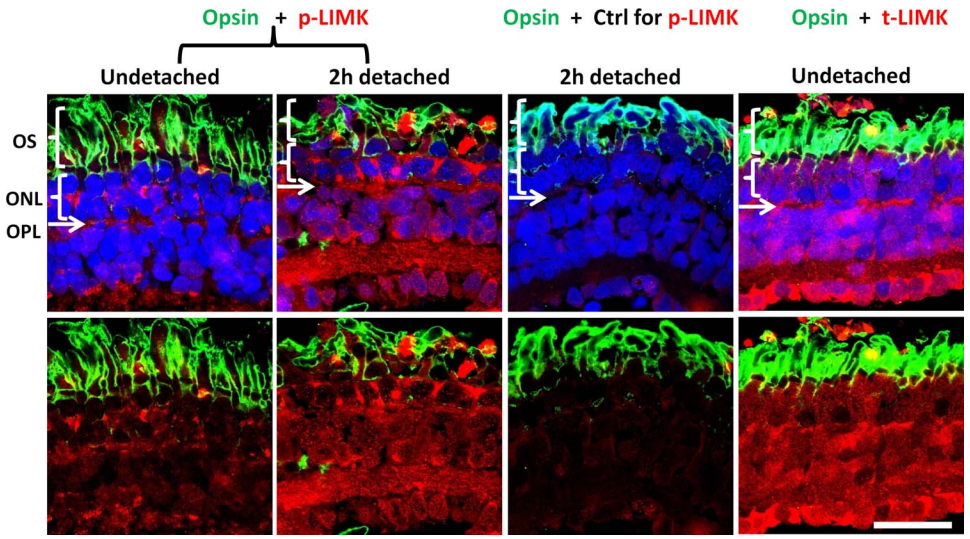

Figure 3. Confocal microscopy demonstrates distribution of LIMK in salamander retina. The outer segments (OS) of rod photoreceptors are labeled for opsin (*green*). The outer nuclear layer (ONL) contains the photoreceptor cell bodies; nuclei are labeled with propidium iodide (*blue*). The outer plexiform layer (OPL) is located immediately beneath the ONL as a thin layer where nuclei are absent. Normal and 2-hour detached retinas, in the *first and second columns*, respectively, are labeled for p-LIMK (*red*); *third column*, a labeling control, anti–p-LIMK is omitted in 2-hour detached retina; *fourth column*, normal retina labeled for t-LIMK (*red*). Labeling of t-LIMK occurs throughout the normal undetached retina; p-LIMK signal is present but spotty in the normal retina and more diffuse, with an apparent increase, in 2-hour detached retina. Optical sections, 1 μm. *Scale bar*: 50 μm. $n = 3$ animals, 2 retinal explants per animal (retina from 1 eye was detached and cultured for 2 hours, retina from other eye was not detached and fixed immediately); 9 cryosections per group (3 cryosections per retinal explant), 2 or 3 images per cryosection.

Investigative Ophthalmology & Visual Science

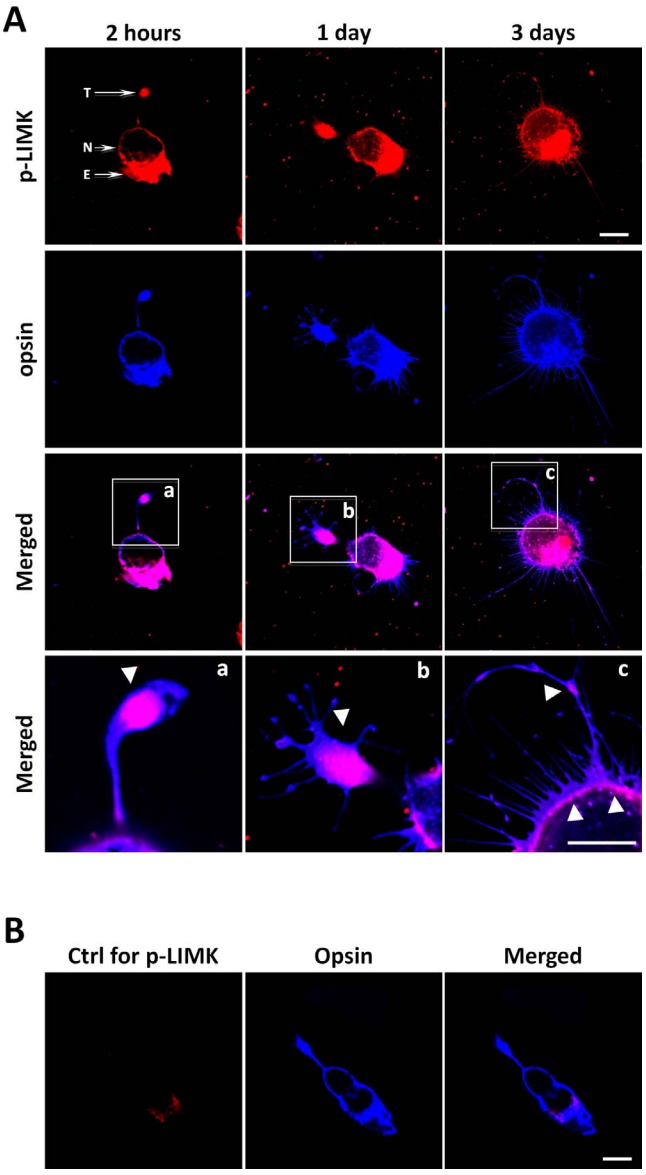

Figure 4. Active LIMK is present in isolated salamander rod cells in culture. (**A**) Rod photoreceptors, which had lost their outer segments, double labeled for p-LIMK (*red*) and rod opsin (*blue*) and examined with confocal microscopy. Labeling occurs throughout the cell except in the nucleus, both during retraction, which occurs during day 1, and after growth of new processes, seen at 3 days. (**a–c**) Enlarged images show the presence of opsin in the cell membrane and p-LIMK in the cytosol and directly under the plasmalemma (*arrowheads*). (**B**) Control for p-LIMK labeling. Rod photoreceptor in 2-hour culture labeled with anti-opsin but without anti–p-LIMK, T, axon terminal; N, nucleus; E, ellipsoid, a collection of mitochondria, in the inner segment. Optical sections, 1 μm. *Scale bars*: 10 μm. $n = 3$ animals, 3 or 4 cultures per animal, 10 to 15 cells imaged per dish (~39 cells per group).

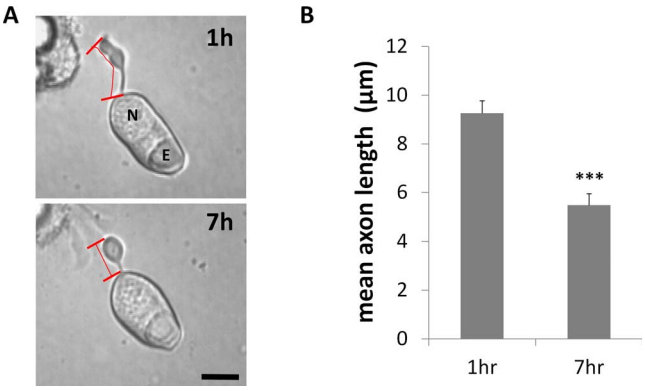

Figure 5. Retraction of rod photoreceptor axon terminals begins during the first 7 hours in culture. (**A**) Representative isolated rod photoreceptor in culture after 1 and 7 hours. Axon length was measured from the base of the cell body to the tip of the axon terminal, shown with *red bars*. N, nucleus; E, ellipsoid. *Scale bar*: 10 μm. (**B**) Mean length of axons was reduced by approximately 40% over 7 hours. $n = 3$ animals, 6 cultures, 59 rod cells, ~30 cells per group; $^{***}P < 0.001$; Student's *t*-test.

Rod Photoreceptor Axonal Retraction in Isolated Cells Is Regulated Through the ROCK-LIMK and Pak-LIMK Pathways

To examine the role of the LIMK pathway in axonal retraction, we applied inhibitors to isolated rod photoreceptors after retinal dissociation and compared their effects on axonal retraction with untreated, control cells. Three inhibitors, Y27632, IPA-3, and BMS-5, were used. Y27632 and IPA-3 are ROCK and Pak inhibitors, respectively,[15,16,54–56] both of which are immediate upstream regulators of LIMK but are themselves activated by different upstream components (Fig. 1). BMS-5 inhibits LIMK activity directly.[32,57,58]

We examined cultures at 7 hours. As rod cell axons are relatively short and 80% of rod cells complete their retraction process within 24 hours after cell plating,[15] 7 hours in culture allows for significant length reduction and yet is before total absorption of the axon into the cell body. In control cultures, treated only with DMSO, rod cell axons shortened noticeably after 7 hours in culture; their axon terminals and cell somas rounded up as well (Fig. 5A). Axon length was reduced 41%, from a mean of 9.3 to 5.5 μm (Fig. 5B).

All three inhibitors prevented axonal retraction in a dose-dependent manner (Figs. 6A–C). The lowest doses used were based on either the reported IC_{50} in solution (IPA-3, 2.5 μM[55]) or previous studies (Y27632[15,16]; BMS-5[32,57]). The highest dose of each inhibitor yielded 50% inhibition compared to the control group. All doses showed no cytotoxicity.

Treatment with Y27632 demonstrated a significant reduction in axonal retraction at the doses above 10 μM (Fig. 6A). These results are consistent with results from our previous study, which showed an increase in the number of cells with a remaining, extended axon, and therefore an inhibition of retraction, after 24 hours.[16] IPA-3 showed a significant reduction of retraction at the doses above 0.7 μM (Fig. 6B). For BMS-5, inhibition was significant at the concentrations greater than 1 μM (Fig. 6C). These results suggest that inhibiting LIMK for up to 7 hours reduces axonal retraction regardless of whether the inhibition is direct or from ROCK- or Pak-associated pathways.

Finally, a combination of ROCK and Pak inhibition demonstrated an additive effect of the RhoA and Rac/Cdc42 pathways. To eliminate the possibility of saturating the inhibitory effect of either ROCK or Pak, we chose low doses of the inhibitors Y27632 and IPA-3 (Figs. 6A, 6B). Y27632 (10 μM) plus IPA-3 (1 μM) decreased axonal retraction to only 40% of the control group value (Fig. 5D). The prevention of retraction by the combined inhibitors was significantly greater than that for either drug at its highest dose alone. Thus both RhoA and Rac/Cdc42 pathways contribute to retraction.

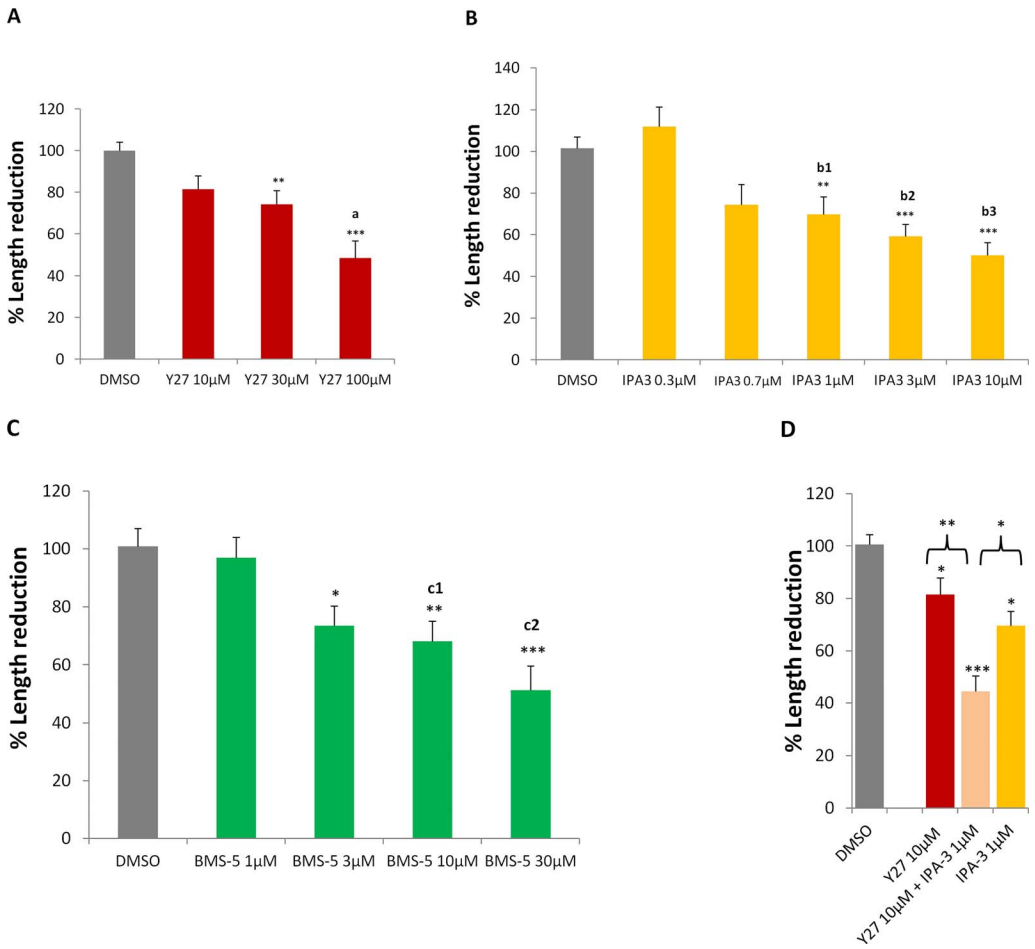

Figure 6. Retraction of the axon is reduced by inhibiting the LIMK pathway. (**A–C**) Inhibiting ROCK or Pak, two different LIMK regulators, or inhibiting LIMK directly, with Y27632 (Y27), IPA-3, or BMS-5, respectively, reduced axonal retraction in a dose-dependent manner. (**D**) Concomitant inhibition of ROCK and Pak with 10 μM Y27632 and 1 μM IPA-3 resulted in significantly more effect on axonal retraction than either treatment alone. % *Length reduction* = $(L1 - L7) \div L1 \times 100\%$; L1, axon length in 1-hour culture; L7, axon length in 7-hour culture. All data were normalized to control (DMSO) group, which is set at 100%. (**A**) $n = 9$ animals, 22 cultures, 411 rod cells, ~100 cells per group. (**B**) $n = 7$ animals, 26 cultures, 483 rod cells, ~80 cells per group. (**C**) $n = 5$ animals, 34 cultures, 430 rod cells, ~86 cells per group. (**D**) $n = 9$ animals, 40 cultures, 502 rod cells, ~126 cells per group. One-way ANOVA, $^{*}P < 0.05$, $^{**}P < 0.01$, $^{***}P < 0.001$; post hoc (Tukey's test), a: Y27 10 vs. 100 μM, $a < 0.05$; b1–b3: IPA3 0.3 vs. 1, 3, or 10 μM, respectively, $b1 < 0.01$, $b2 < 0.001$, $b3 < 0.001$; c1, c2: BMS-5 1 vs. 10 or 30 μM, respectively, $c1 < 0.05$, $c2 < 0.01$.

The Effect of LIMK Inhibition on Rod Cell Axonal Retraction Is Not Increased by a Ca^{2+} Channel Blocker

Influx of Ca^{2+} through L-type channels has been described as necessary for retraction in salamander rod cells[18]; its effect is likely due to activation of MLCK to promote actomyosin contraction (Fig. 1).[16,59,60] Here we applied the channel blocker nicardipine (Nc) alone or in the presence of ROCK or LIMK inhibitors to examine how reduction in Ca^{2+} influx together with decreased LIMK or ROCK activity affects axonal retraction. We used 10 μM Nc to be consistent with previous studies.[16,18]

Y27632 (10 μM) plus Nc (10 μM) resulted in more inhibition of retraction than Y27632 (10 μM) alone (Fig. 7). When 30 μM Y27632 plus Nc (10 μM) was applied, inhibition increased and resulted in more inhibition of retraction than either Y27632 (30 μM) or Nc (10 μM) alone (Fig. 7). These data are consistent with our proposed pathways for regulation of photoreceptor axonal and neuritic plasticity (Fig. 1) in which ROCK activates multiple effectors, LIMK, MLC, and MLCP, whereas Ca^{2+} signaling activates MLCK to promote axonal retraction. ROCK and Ca^{2+} together would reasonably be expected to increase actomyosin contraction by increasing the number of activated effectors.

We also examined the effect of BMS-5 (10 μM) plus Nc (10 μM) treatment. In contrast to ROCK inhibition, LIMK inhibition plus Ca^{2+} blockage did not result in any further effect (Fig. 7). This suggests a complex relationship between Ca^{2+} signaling and LIMK activity, which will be discussed below.

LIMK Inhibition Prevents Rod Cell Process Growth and the Effect Is Enhanced With Nicardipine Treatment

In vitro, neuritic sprouting by rod cells closely follows retraction. As previously described,[48] filopodial processes are present by 24 hours of culture; some filopodia elongate and become thicker neuritic processes by 3 days (Fig. 4A). The growth is similar to rod cell sprouting seen in retinal disease and after retinal reattachment.[3,5,7,15,17,38,48,61] Here we assessed the effect of LIMK or Pak inhibition on process growth after 3 days in culture.

Growth was examined for each cell as a whole and for the basal (nuclear) and apical (ellipsoidal) poles separately. Photoreceptors are highly polarized cells. They have different

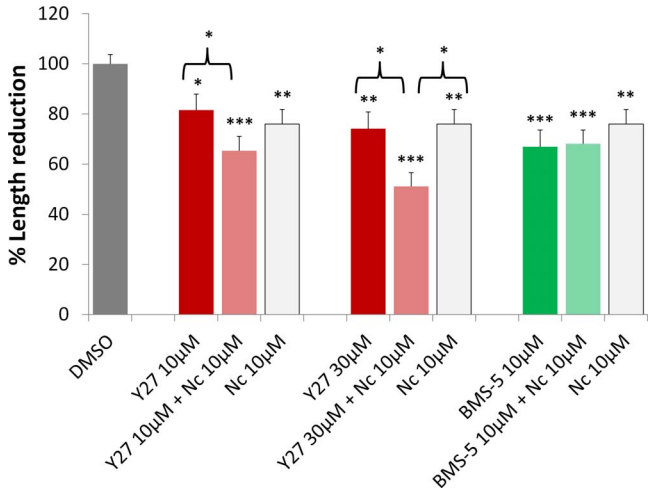

Figure 7. Blockage of Ca^{2+} influx increases the effect of ROCK inhibition on axonal retraction over 7 hours, but does not affect LIMK inhibition. 10 μM nicardipine (Nc), an L-type Ca^{2+} channel blocker, reduced axonal retraction; 10 μM Nc plus Y27632 (Y27), a ROCK inhibitor, at 10 or 30 μM, had significantly more effect on reducing axonal retraction than Y27632 treatment alone. Ten μM Nc plus 10 μM BMS-5, a LIMK inhibitor, did not demonstrate an additional effect on retraction over Nc or BMS-5 treatment alone. Analysis of length was the same as in Figure 6. $n = 10$ animals, 64 cultures, 957 rod cells, ~95 cells per group; $^{*}P < 0.05$, $^{**}P < 0.01$, $^{***}P < 0.001$; 1-way ANOVA between DMSO and (Y2710 μM, Y2710 μM + Nc10 μM, Nc 10μM), or (Y27 30 μM, Y27 30 μM + Nc 10 μM, Nc 10 μM), or (BMS-5 10 μM, BMS-5 10 μM + Nc 10 μM, Nc 10 μM).

kinds of processes that emerge from their two ends, axon processes from the nuclear/basal pole and calycal processes (filopodial-like processes that normally surround the base of the outer segment) from the ellipsoidal/apical pole (Fig. 8A, left). In the control group, the average length of the longest process originating from any point on the cell's circumference (designated the overall group), was 27 μm after 3 days in culture, whereas processes from the nuclear and ellipsoidal poles were 20 μm long on average (Figs. 8B, 8C). The overall average length was longer than either of the regional process lengths because the longest process from each cell does not consistently originate from either pole.

Treatment with IPA-3 (1 μM) reduced process growth in all three groups (Fig. 8B), the overall, the nuclear, and the ellipsoidal poles, with the basal processes significantly shorter with IPA-3 treatment than the apical processes. Thus, Pak activity, which is involved in retraction, continues to be involved when rod cells begin the later stage of neuritic growth. Treatment with BMS-5 (10 μM) also reduced overall growth (Fig. 8C); however, when examining the separate regions of the rod cell, it was clear that while basal process growth was reduced, there was no significant effect on processes from the apical pole (Fig. 8C).

These data suggest that basal processes are more sensitive to regulation by the LIMK pathway than apical processes. Effects on the basal processes are consistent with results shown in Figure 4A (1 and 3 days), which demonstrated that the localization of p-LIMK is enriched in the axon processes (arrowheads) and suggests that there is continuous activity of p-LIMK in the axonal region of rod photoreceptors during both axonal retraction and process outgrowth.

For growth, in contrast to the results on retraction, simultaneous application of a LIMK inhibitor and Nc further reduced rod cell outgrowth in both nuclear and ellipsoid regions (Fig. 8C). Thus, LIMK and Ca^{2+} inhibition demonstrated a different relationship after 3 days in culture during process outgrowth than after 7 hours in culture during axonal retraction.

Inhibition of LIMK Prevents Photoreceptor Axonal Retraction After Retinal Detachment

To examine whether the LIMK signaling pathway is active in rod photoreceptors in the intact retina after injury, we analyzed axonal retraction by rod photoreceptors after detachment of porcine retina. Porcine retina shares similarities with human retina in terms of anatomy, vasculature, and photoreceptor distribution.[42–46] These features make this animal model useful for translational experiments.

After detachment, retinal explants were incubated with or without BMS-5 (10 μM). Since previous studies in our lab had shown significant structural change after 24-hour incubation compared to normal retina,[16] here we examined the effect of LIMK inhibition in retina detached for 24 hours.

In normal, healthy retina, SV2 labeling forms a bright band in the OPL layer where synaptic connections between photoreceptors and horizontal and bipolar cells occur.[16] When rod cell axons retract, SV2 signal shows up in the ONL region where photoreceptor cell bodies reside.[16,51] With confocal microscopy, we observed prominent SV2 signal in the ONL after 24 hours (Fig. 9A, left column). This is not ascribed to a defect in vesicle localization because previous studies, using opsin labeling, showed that the cell plasma membrane retreats along with synaptic protein.[51] Thus prominent SV2 label in the ONL indicates retraction of synaptic terminals. BMS-5–treated retina had significantly less SV2 staining in the ONL (Fig. 9A, right column; Fig. 9B). This result demonstrated that inhibition of LIMK reduces axonal retraction of rod photoreceptor after injury in mammalian retina.

Treatment with BMS-5 also seemed to affect the general morphology of the retina. Culture of detached retina often promotes an increase in the width of the ONL, presumably the result of structural loosening. With LIMK inhibition, the width of the ONL was 10% less than that of the control group (39.3 ± 2.18 vs. 43.7 ± 1.79 μm; $n = 3$ animals). Although not statistically significant, this suggests closer cell–cell and cell–matrix contact. Furthermore, the OPL appeared to be more organized and linear and the SV2 label more intense and compact (Fig. 9A). This suggests that LIMK inhibition may also help retain retinal morphology after detachment. In conclusion, both in single cells and in mammalian retina, LIMK inhibition significantly reduced axonal retraction in response to injury.

Discussion

The LIMK family, which includes LIMK1 and LIMK2, is involved in a variety of physiological and pathologic activities through its regulation of actin, and possibly microtubule, cytoskeletal dynamics. For instance, LIMK has been reported to be important for regulating axon guidance of retinal ganglion cells and photoreceptors during development[29,62–64] and in central nervous system (CNS) synaptic plasticity.[24,65–67] In the case of retinal detachment, rod photoreceptors retract their synaptic terminals back to the cell body immediately after injury and show neuritic sprouting at later stages in response to reattachment.[5,7,38] The dramatic morphologic change of the axonal and presynaptic region suggests increased actin filament turnover and significant structural change in the actin cytoskeleton. Our previous studies demonstrated that RhoA-ROCK activity regulated synaptic plasticity in rod photoreceptors: Inhibition of ROCK blocked retraction of photoreceptor

Investigative Ophthalmology & Visual Science

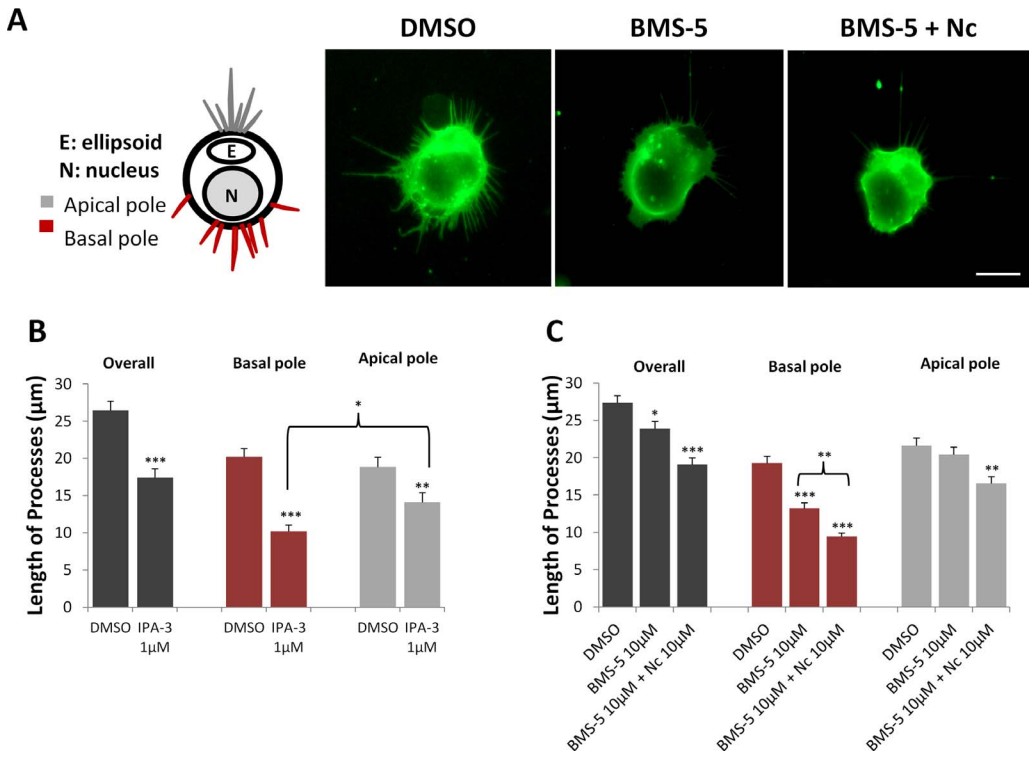

Figure 8. Growth of processes by rod cells is reduced with Pak or LIMK inhibition; blockage of Ca^{2+} influx furthers the effect of LIMK inhibition. (**A**) *Left*: Cartoon of regional designations for rod cell processes. In the intact retina, axonal processes grow from the basal/nuclear pole, whereas calycal processes that surround the outer segment grow from the apical/ellipsoidal pole. *Right*: Representative rod cells with rod opsin labeling from DMSO control, 10 µM BMS-5-, and 10 µM Nc plus 10 µM BMS-5-treated cultures after 3 days. Cells in control, untreated cultures show the most growth. *Scale bar*: 10 µm. (**B**) Length of the longest process from three regions (overall, longest process regardless of region of origin; basal, from the cell surface close to the nucleus; apical, from the cell surface close to the ellipsoid) of each rod cell. Pak inhibition with 1 µM IPA-3 reduced process growth of rod cells after 3 days in culture from all regions, compared to control. In control cells, length of apical and basal processes is similar; in IPA-3-treated group, basal processes shortened significantly more than apical processes. $n = 3$ animals, 12 cultures, 360 rod cells, ~180 cells per group; $^{*}P < 0.05$, $^{**}P < 0.005$. (**C**) LIM kinase inhibition with 10 µM BMS-5 reduced process growth overall and from the basal but not the apical pole. Blockage of Ca^{2+} influx increased the effect of LIMK inhibition and reduced process growth from basal and apical regions. $n = 3$ animals, 18 cultures, 540 rod cells, ~180 cells per group; $^{*}P < 0.05$, $^{**}P < 0.01$, $^{***}P < 0.001$; (**B**) Student's *t*-test; (**C**) 1-way ANOVA.

axons after retinal detachment.[15,16] Since ROCK is one of the major regulators of LIMK, and because LIMK is involved in actin dynamics, we hypothesized that LIMK contributes to axonal retraction and process outgrowth of photoreceptors after injury by increasing actin filament turnover. Our results provide evidence in support of this hypothesis.

The presence of LIMK activity in retina was demonstrated with Western blot and immunocytochemistry. With confocal microscopy we observed the localization of p-LIMK in rod axon terminals, precisely the area that undergoes dramatic morphologic change after retinal dissociation. Measuring the reduction in axon length allowed us to demonstrate the prevention of axonal retraction by inhibiting LIMK. Furthermore, inhibiting LIMK upstream regulators, ROCK and Pak, increased inhibition of axonal retraction, and the two pathways demonstrated an additive effect. The involvement of ROCK is not surprising, as we have previously demonstrated that inhibiting the RhoA-ROCK pathway can block axonal retraction.[15,16] ROCK has been reported to be responsible for actomyosin contractility as well as actin filament turnover (Fig. 1).[19,20,35–37] Blocking its activity therefore presumably reduces both contraction and actin filament turnover. Pak has been reported to regulate formation of filopodia and lamellipodia via the Rac and Cdc42 pathways, respectively.[19,20,35–37] The role of Rac and Cdc42 in promoting growth is achieved through actin filament nucleation by ARP2/3 and Pak activities.[39–41] We speculate that the role of Pak in retraction may be to promote depolymerization of actin filaments through LIMK activity. Such depolymerization would be necessary to form new actin cytoskeleton in either filopodia or lamellipodia. Thus inhibiting Pak may result in less disassembly, and less turnover, of the actin cytoskeleton and hence reduced axonal retraction in our study. The enhanced inhibition of axonal retraction by combining ROCK and Pak is consistent with our hypothesized mechanism (Fig. 1) if we assume that neither drug, at the dosages used, is able to maximally inhibit LIMK. However, enhanced inhibition by combining ROCK and Pak inhibitors could conceivably occur if each is working along an independent pathway. Definitive evidence of the convergence of ROCK and Pak onto LIMK in rod cells remains to be demonstrated.

With longer times in vitro, the presynaptic remodeling of the rod photoreceptor moves from axonal retraction to the formation of neuritic processes. In the intact retina, sprouting may be as destructive as axonal retraction to vision because neuritic processes in retina grow beyond the OPL layer, where the normal synaptic connection between photoreceptors and horizontal or bipolar cells is located, and hence disrupt normal circuitry.[4,68–70] Either LIMK or Pak inhibition resulted in less process growth from the axonal region, the basal/nuclear pole, of the rod cell. In contrast, ROCK inhibition in previous studies showed no effect on process growth.[15]

Based on the above results, we propose that LIMK is a better therapeutic target than either ROCK or Pak for

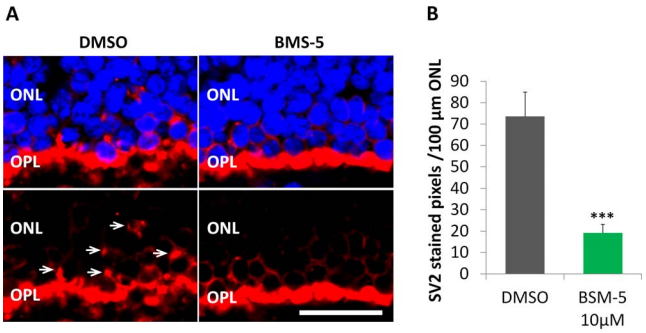

Figure 9. Inhibition of LIMK reduces axonal retraction in the porcine retina maintained in vitro for 24 hours after detachment. (**A**) Representative control and treated retinas after 24 hours in vitro. The outer plexiform layer (OPL) with rod synaptic terminals is labeled for synaptic vesicles, SV2 (*red*). The outer nuclear layer (ONL) contains the photoreceptor cell bodies; nuclei are labeled with propidium iodide (*blue*). *Left*: With no treatment, SV2 label is present among the photoreceptor cell bodies (*arrows*) indicating that the rod terminals have retracted. *Right*: Treatment with 10 µM BMS-5, a LIMK inhibitor, reduced the level of SV2 in the ONL indicating an inhibition of retraction. *Scale bar*: 10 µm. (**B**) Retraction is measured using the area of SV2 label in the ONL. Treatment with 10 µM BMS-5 reduced SV2 labeling in the ONL significantly, compared to untreated retinas. Optical sections, 1 µm. $n = 3$ animals, 2 retinal explants per animal (1 explant with BMS-5 treatment from one eye, the other explant with DMSO as control from the other eye); 7 cryosections per group (2 or 3 cryosections per retinal explant), 3 or 4 images per cryosection. $^{***}P < 0.001$; Student's *t*-test.

preservation of the normal synaptic structure of rod photoreceptors after retinal detachment. The advantage of LIMK inhibition lies in its ability to reduce both axonal retraction and neuritic sprouting, potentially through stabilizing cytoskeletal structure. ROCK inhibition, in addition to showing no effect on reducing neuritic sprouting, actually promotes varicosity development in the processes.[5] Since varicosity formation implies functional presynaptic terminals, ROCK inhibition could potentially promote additional synaptic activity. Although Pak reduces both retraction and sprouting, as an upstream regulator of LIMK, it activates other effectors and hence is involved in other functions, such as cell survival, gene transcription, and hormone signaling.[71–79] Pak inhibition therefore may affect several rod photoreceptor physiological activities, whereas LIMK effectors are mainly involved in regulating cytoskeleton dynamics and LIMK inhibition therefore may have a more focused effect.

The therapeutic function of LIMK inhibition was tested and confirmed in porcine retina, which mimics human retina structurally and physiologically. Twenty-four hours after detachment, porcine retina treated with a LIMK inhibitor demonstrated significantly less synaptic retraction by rod photoreceptors than retinas with no treatment. Furthermore, LIMK inhibition also appeared to improve the morphology of the retina in general. This may be due to effects on adherens junctions that form a zonular attachment between photoreceptors and Müller cells.[80] Studies have revealed the involvement of both RhoA and Rac pathways in endothelial barrier dysfunction and hyperpermeability through regulation of adherens junctions.[81–86] It was also reported that the ROCK-LIMK pathway regulates adherens junction dynamics between Sertoli and germ cells during spermatogenesis.[87] In detached retina, upregulated activity of the LIMK pathway will increase the dynamics of actin filaments and hence is likely to disrupt adherens junctions and loosen cell–cell connections. LIM kinase inhibition would reduce these changes and achieve overall structural stability of detached retina.

The dual therapeutic benefits of LIMK inhibition also revealed that the two seemingly opposite responses, axon retraction and neurite outgrowth, share a common mechanism through LIMK: Both require turnover of actin filaments. The direction of synaptic morphologic changes, to retract or to sprout, may depend on the balance of actin depolymerization and polymerization, the latter being regulated by Rac/Cdc42 pathways as stated above.[39–41] In our study, the contribution of Pak to both retraction and growth suggests that although process growth in isolated rod cells appears to be a late-stage development, the Rac/Cdc42 growth pathways may be activated early on. However, when and where actin filament nucleation and elongation begins still needs to be examined. While we demonstrate here that LIMK serves as a coordinator, more studies are required to define the temporal and spatial relationship between other potential players that contribute to actin filament turnover during presynaptic structural plasticity of the rod photoreceptor in response to injury.

Although our hypothesized mechanism focuses on regulation of actin dynamics by LIMK, the process of axonal retraction in rod photoreceptor involves another important cytoskeletal structure, microtubules. Microtubules support the axonal shaft, whereas actin filaments are enriched in axon terminals. When the axon terminal retracts, shortening of the axon occurs concurrently. This strongly suggests that microtubules depolymerize during retraction. LIM kinase inhibition may stabilize microtubules. There are two possible mechanisms, indirectly by reduced tension between actin filaments and microtubules,[88–90] and directly by reduced LIMK-promoted microtubule depolymerization.[91–95] However, the stabilization of microtubules in axons of rod cells with inhibition of the LIMK pathway remains to be tested.

Another interesting player in the regulation of photoreceptor presynaptic remodeling is Ca^{2+}. In our 7-hour experiments, combining ROCK inhibition and L-type Ca^{2+} channel blockage demonstrated significantly more effect than either treatment alone. A likely explanation involves the downregulation of actomyosin contractile force; Ca^{2+}-calmodulin promotes actomysion contraction through activating MLCK, and ROCK achieves the same effect through phosphorylating MLC and MLCP.

Combining LIMK inhibition with Ca^{2+} channel blockage, however, had no increased effect on retraction. As our proposed mechanism indicates (Fig. 1), inhibiting LIMK and Ca^{2+} influx does not affect the signaling pathway from ROCK to MLC or MLCP, which will upregulate actomyosin contraction. Thus, LIMK inhibition plus blockage of Ca^{2+} influx does not prevent axonal retraction due to active actomyosin contraction. ROCK inhibition plus blockage of Ca^{2+} influx, on the other hand, affects all immediate components needed for actomysion contraction as well as actin filament turnover. In addition, the relationship between the LIMK-cofilin pathway and Ca^{2+} is not well understood and has been reported to vary under different circumstances in neurons.[96,97]

In contrast to the 7-hour retraction data, at 3 days in culture, a period when process outgrowth occurs, combined LIMK inhibition and Ca^{2+} influx blockage showed significantly further inhibition than LIMK inhibition alone. As actomyosin contraction is unlikely to contribute to process growth directly, one possible role of Ca^{2+} signaling in neuritic growth is that elevated intracellular Ca^{2+} upregulates LIMK activity through a Ca^{2+}-calmodulin-CaMKIV-LIMK signaling pathway.[97] Additionally, slingshot (SSH), the major phosphatase for cofilin, has been reported to be under regulation by Ca^{2+} signaling.[98,99] Thus, it is also possible that under combined treatments, the phosphatase (SSH) activity increased due to Ca^{2+} blockage by Nc while the kinase (LIMK) activity was inhibited directly by

BMS-5. More research is required to understand the role of Ca^{2+}, especially its microdomain specificity, and spatial and temporal relationships with LIMK-cofilin, SSH-cofilin, and the MLC pathway.

Previous studies have demonstrated LIMK pathway activity during axon guidance in developing CNS.[62–64] Our study reports a role for LIMK in adult neurons as well, during structural remodeling of rod cell axon terminals after mechanical injury. Our findings further suggest that there may be a therapeutic benefit in inhibiting LIMK after retinal detachment. By preventing both axonal retraction and neuritic sprouting, the retinal circuitry may be stabilized.

Acknowledgments

The authors thank Jianfeng Wang for assistance with immunohistochemical analysis and Ilene Sugino for assistance with confocal microscopy.

Supported by National Institutes of Health Grant EY021542 and the F.M. Kirby Foundation.

Disclosure: **W. Wang**, None; **E. Townes-Anderson**, None

References

1. Erickson PA, Fisher SK, Anderson DH, Stern WH, Borgula GA. Retinal detachment in the cat: the outer nuclear and outer plexiform layers. *Invest Ophthalmol Vis Sci*. 1983;24:927–942.
2. Lewis GP, Linberg KA, Fisher SK. Neurite outgrowth from bipolar and horizontal cells after experimental retinal detachment. *Invest Ophthalmol Vis Sci*. 1998;39:424–434.
3. Li ZY, Kljavin IJ, Milam AH. Rod photoreceptor neurite sprouting in retinitis pigmentosa. *J Neurosci*. 1995;15:5429–5438.
4. Milam AH, Li ZY, Cideciyan AV, Jacobson SG. Clinicopathologic effects of the Q64ter rhodopsin mutation in retinitis pigmentosa. *Invest Ophthalmol Vis Sci*. 1996;37:753–765.
5. Lewis GP, Charteris DG, Sethi CS, Fisher SK. Animal models of retinal detachment and reattachment: identifying cellular events that may affect visual recovery. *Eye (Lond)*. 2002;16:375–387.
6. Gupta N, Brown KE, Milam AH. Activated microglia in human retinitis pigmentosa, late-onset retinal degeneration, and age-related macular degeneration. *Exp Eye Res*. 2003;76:463–471.
7. Sethi CS, Lewis GP, Fisher SK, et al. Glial remodeling and neural plasticity in human retinal detachment with proliferative vitreoretinopathy. *Invest Ophthalmol Vis Sci*. 2005;46:329–342.
8. Fisher SK, Stone J, Rex TS, Linberg KA, Lewis GP. Experimental retinal detachment: a paradigm for understanding the effects of induced photoreceptor degeneration. *Prog Brain Res*. 2001;131:679–698.
9. Tielsch JM, Legro MW, Cassard SD, et al. Risk factors for retinal detachment after cataract surgery. A population-based case-control study. *Ophthalmology*. 1996;103:1537–1545.
10. Yorston D, Jalali S. Retinal detachment in developing countries. *Eye (Lond)*. 2002;16:353–358.
11. Gariano RF, Kim CH. Evaluation and management of suspected retinal detachment. *Am Fam Physician*. 2004;69:1691–1698.
12. Haug SJ, Bhisitkul RB. Risk factors for retinal detachment following cataract surgery. *Curr Opin Ophthalmol*. 2012;23:7–11.
13. Feltgen N, Walter P. Rhegmatogenous retinal detachment–an ophthalmologic emergency. *Dtsch Arztebl Int*. 2014;111:12–21, quiz 22.
14. Johnston PB. Traumatic retinal detachment. *Br J Ophthalmol*. 1991;75:18–21.
15. Fontainhas AM, Townes-Anderson E. RhoA and its role in synaptic structural plasticity of isolated salamander photoreceptors. *Invest Ophthalmol Vis Sci*. 2008;49:4177–4187.
16. Fontainhas AM, Townes-Anderson E. RhoA inactivation prevents photoreceptor axon retraction in an in vitro model of acute retinal detachment. *Invest Ophthalmol Vis Sci*. 2011;52:579–587.
17. Zhang N, Townes-Anderson E. Regulation of structural plasticity by different channel types in rod and cone photoreceptors. *J Neurosci*. 2002;22:7065–7079.
18. Nachman-Clewner M, St Jules R, Townes-Anderson E. L-type calcium channels in the photoreceptor ribbon synapse: localization and role in plasticity. *J Comp Neurol*. 1999;415:1–16.
19. Maekawa M, Ishizaki T, Boku S, et al. Signaling from Rho to the actin cytoskeleton through protein kinases ROCK and LIM-kinase. *Science*. 1999;285:895–898.
20. Bito H, Furuyashiki T, Ishihara H, et al. A critical role for a Rho-associated kinase, p160ROCK, in determining axon outgrowth in mammalian CNS neurons. *Neuron*. 2000;26:431–441.
21. Ng J, Luo L. Rho GTPases regulate axon growth through convergent and divergent signaling pathways. *Neuron*. 2004;44:779–793.
22. Koth AP, Oliveira BR, Parfitt GM, Buonocore Jde Q, Barros DM. Participation of group I p21-activated kinases in neuroplasticity. *J Physiol Paris*. 2014;108:270–277.
23. Edwards DC, Sanders LC, Bokoch GM, Gill GN. Activation of LIM-kinase by Pak1 couples Rac/Cdc42 GTPase signalling to actin cytoskeletal dynamics. *Nat Cell Biol*. 1999;1:253–259.
24. Yang EJ, Yoon JH, Min DS, Chung KC. LIM kinase 1 activates cAMP-responsive element-binding protein during the neuronal differentiation of immortalized hippocampal progenitor cells. *J Biol Chem*. 2004;279:8903–8910.
25. Edwards DC, Gill GN. Structural features of LIM kinase that control effects on the actin cytoskeleton. *J Biol Chem*. 1999;274:11352–11361.
26. Welch MD, Mallavarapu A, Rosenblatt J, Mitchison TJ. Actin dynamics in vivo. *Curr Opin Cell Biol*. 1997;9:54–61.
27. Foletta VC, Moussi N, Sarmiere PD, Bamburg JR, Bernard O. LIM kinase 1, a key regulator of actin dynamics, is widely expressed in embryonic and adult tissues. *Exp Cell Res*. 2004;294:392–405.
28. Manetti F. LIM kinases are attractive targets with many macromolecular partners and only a few small molecule regulators. *Med Res Rev*. 2012;32:968–998.
29. Montani L, Gerrits B, Gehrig P, et al. Neuronal Nogo-A modulates growth cone motility via Rho-GTP/LIMK1/cofilin in the unlesioned adult nervous system. *J Biol Chem*. 2009;284:10793–10807.
30. Yang Q, Zhang XF, Van Goor D, et al. Protein kinase C activation decreases peripheral actin network density and increases central nonmuscle myosin II contractility in neuronal growth cones. *Mol Biol Cell*. 2013;24:3097–3114.
31. Craig EM, Van Goor D, Forscher P, Mogilner A. Membrane tension, myosin force, and actin turnover maintain actin treadmill in the nerve growth cone. *Biophys J*. 2012;102:1503–1513.
32. Scott RW, Hooper S, Crighton D, et al. LIM kinases are required for invasive path generation by tumor and tumor-associated stromal cells. *J Cell Biol*. 2010;191:169–185.
33. Hopkins AM, Pineda AA, Winfree LM, Brown GT, Laukoetter MG, Nusrat A. Organized migration of epithelial cells requires control of adhesion and protrusion through Rho kinase effectors. *Am J Physiol Gastrointest Liver Physiol*. 2007;292:G806–G817.
34. Kidera Y, Tsubaki M, Yamazoe Y, et al. Reduction of lung metastasis, cell invasion, and adhesion in mouse melanoma by

statin-induced blockade of the Rho/Rho-associated coiled-coil-containing protein kinase pathway. *J Exp Clin Cancer Res*. 2010;29:127.

35. Nakai K, Suzuki Y, Kihira H, et al. Regulation of myosin phosphatase through phosphorylation of the myosin-binding subunit in platelet activation. *Blood*. 1997;90:3936–3942.
36. Totsukawa G, Yamakita Y, Yamashiro S, Hartshorne DJ, Sasaki Y, Matsumura F. Distinct roles of ROCK (Rho-kinase) and MLCK in spatial regulation of MLC phosphorylation for assembly of stress fibers and focal adhesions in 3T3 fibroblasts. *J Cell Biol*. 2000;150:797–806.
37. Julian L, Olson MF. Rho-associated coiled-coil containing kinases (ROCK): structure, regulation, and functions. *Small GTPases*. 2014;5:e29846.
38. Lewis GP, Fisher SK. Up-regulation of glial fibrillary acidic protein in response to retinal injury: its potential role in glial remodeling and a comparison to vimentin expression. *Int Rev Cytol*. 2003;230:263–290.
39. Li Y, Wang PS, Lucas G, Li R, Yao L. ARP2/3 complex is required for directional migration of neural stem cell-derived oligodendrocyte precursors in electric fields. *Stem Cell Res Ther*. 2015;6:41.
40. Courtemanche N, Gifford SM, Simpson MA, Pollard TD, Koleske AJ. Abl2/Abl-related gene stabilizes actin filaments, stimulates actin branching by actin-related protein 2/3 complex, and promotes actin filament severing by cofilin. *J Biol Chem*. 2015;290:4038–4046.
41. Helgeson LA, Prendergast JG, Wagner AR, Rodnick-Smith M, Nolen BJ. Interactions with actin monomers, actin filaments, and Arp2/3 complex define the roles of WASP family proteins and cortactin in coordinately regulating branched actin networks. *J Biol Chem*. 2014;289:28856–28869.
42. Arevalo JF, Sanchez JG, Saldarriaga L, et al. Retinal detachment after bevacizumab. *Ophthalmology*. 2011;118:2304, e2303–e2307.
43. Middleton S. Porcine ophthalmology. *Vet Clin North Am Food Anim Pract*. 2010;26:557–572.
44. Pennesi ME, Neuringer M, Courtney RJ. Animal models of age related macular degeneration. *Mol Aspects Med*. 2012;33:487–509.
45. Lassota N, Kiilgaard JF, Prause JU, Qvortrup K, Scherfig E, la Cour M. Surgical induction of choroidal neovascularization in a porcine model. *Graefes Arch Clin Exp Ophthalmol*. 2007;245:1189–1198.
46. Lassota N, Prause JU, Scherfig E, Kiilgaard JF, la Cour M. Clinical and histological findings after intravitreal injection of bevacizumab (Avastin) in a porcine model of choroidal neovascularization. *Acta Ophthalmol*. 2010;88:300–308.
47. MacLeish PR, Townes-Anderson E. Growth and synapse formation among major classes of adult salamander retinal neurons in vitro. *Neuron*. 1988;1:751–760.
48. Mandell JW, MacLeish PR, Townes-Anderson E. Process outgrowth and synaptic varicosity formation by adult photoreceptors in vitro. *J Neurosci*. 1993;13:3533–3548.
49. Nachman-Clewner M, Townes-Anderson E. Injury-induced remodelling and regeneration of the ribbon presynaptic terminal in vitro. *J Neurocytol*. 1996;25:597–613.
50. MacLeish PR, Barnstable CJ, Townes-Anderson E. Use of a monoclonal antibody as a substrate for mature neurons in vitro. *Proc Natl Acad Sci U S A*. 1983;80:7014–7018.
51. Khodair MA, Zarbin MA, Townes-Anderson E. Synaptic plasticity in mammalian photoreceptors prepared as sheets for retinal transplantation. *Invest Ophthalmol Vis Sci*. 2003;44:4976–4988.
52. Hiraoka J. Identification and characterization of a novel family of serine/threonine kinases containing two N-terminal LIM motifs. *J Biol Chem*. 1995;270:31321–31330.
53. Alfinito PD, Townes-Anderson E. Activation of mislocalized opsin kills rod cells: a novel mechanism for rod cell death in retinal disease. *Proc Natl Acad Sci U S A*. 2002;99:5655–5660.
54. Takahashi K, Suzuki K. Membrane transport of WAVE2 and lamellipodia formation require Pak1 that mediates phosphorylation and recruitment of stathmin/Op18 to Pak1-WAVE2-kinesin complex. *Cell Signal*. 2009;21:695–703.
55. Deacon SW, Beeser A, Fukui JA, et al. An isoform-selective, small-molecule inhibitor targets the autoregulatory mechanism of p21-activated kinase. *Chem Biol*. 2008;15:322–331.
56. Uehata M, Ishizaki T, Satoh H, et al. Calcium sensitization of smooth muscle mediated by a Rho-associated protein kinase in hypertension. *Nature*. 1997;389:990–994.
57. Petrilli A, Copik A, Posadas M, et al. LIM domain kinases as potential therapeutic targets for neurofibromatosis type 2. *Oncogene*. 2014;33:3571–3582.
58. Ross-Macdonald P, de Silva H, Guo Q, et al. Identification of a nonkinase target mediating cytotoxicity of novel kinase inhibitors. *Mol Cancer Ther*. 2008;7:3490–3498.
59. Means AR. Regulatory cascades involving calmodulin-dependent protein kinases. *Mol Endocrinol*. 2000;14:4–13.
60. Braun AP, Schulman H. The multifunctional calcium/calmodulin-dependent protein kinase: from form to function. *Annu Rev Physiol*. 1995;57:417–445.
61. Kljavin IJ, Reh TA. Muller cells are a preferred substrate for in vitro neurite extension by rod photoreceptor cells. *J Neurosci*. 1991;11:2985–2994.
62. Strochlic L, Dwivedy A, van Horck FP, Falk J, Holt CE. A role for S1P signalling in axon guidance in the Xenopus visual system. *Development*. 2008;135:333–342.
63. Hocking JC, Hehr CL, Bertolesi G, Funakoshi H, Nakamura T, McFarlane S. LIMK1 acts downstream of BMP signaling in developing retinal ganglion cell axons but not dendrites. *Dev Biol*. 2009;330:273–285.
64. Hing H, Xiao J, Harden N, Lim L, Zipursky SL. Pak functions downstream of Dock to regulate photoreceptor axon guidance in Drosophila. *Cell*. 1999;97:853–863.
65. Heredia L, Helguera P, de Olmos S, et al. Phosphorylation of actin-depolymerizing factor/cofilin by LIM-kinase mediates amyloid beta-induced degeneration: a potential mechanism of neuronal dystrophy in Alzheimer's disease. *J Neurosci*. 2006;26:6533–6542.
66. Koch JC, Tonges L, Barski E, Michel U, Bahr M, Lingor P. ROCK2 is a major regulator of axonal degeneration, neuronal death and axonal regeneration in the CNS. *Cell Death Dis*. 2014;5:e1225.
67. Piccioli ZD, Littleton JT. Retrograde BMP signaling modulates rapid activity-dependent synaptic growth via presynaptic LIM kinase regulation of cofilin. *J Neurosci*. 2014;34:4371–4381.
68. Marc RE, Jones BW, Watt CB, Strettoi E. Neural remodeling in retinal degeneration. *Prog Retin Eye Res*. 2003;22:607–655.
69. Banin E, Cideciyan AV, Aleman TS, et al. Retinal rod photoreceptor-specific gene mutation perturbs cone pathway development. *Neuron*. 1999;23:549–557.
70. Fisher SK, Lewis GP, Linberg KA, Verardo MR. Cellular remodeling in mammalian retina: results from studies of experimental retinal detachment. *Prog Retin Eye Res*. 2005;24:395–431.
71. Zins K, Gunawardhana S, Lucas T, Abraham D, Aharinejad S. Targeting Cdc42 with the small molecule drug AZA197 suppresses primary colon cancer growth and prolongs survival in a preclinical mouse xenograft model by downregulation of PAK1 activity. *J Transl Med*. 2013;11:295.
72. Zhao Z, Park C, McDevitt MA, et al. p21-Activated kinase mediates rapid estradiol-negative feedback actions in the reproductive axis. *Proc Natl Acad Sci U S A*. 2009;106:7221–7226.

Investigative Ophthalmology & Visual Science

73. Yeo D, He H, Baldwin GS, Nikfarjam M. The role of p21-activated kinases in pancreatic cancer. *Pancreas*. 2015;44:363–369.
74. Tao J, Oladimeji P, Rider L, Diakonova M. PAK1-Nck regulates cyclin D1 promoter activity in response to prolactin. *Mol Endocrinol*. 2011;25:1565–1578.
75. Rane CK, Minden A. P21 activated kinases: structure, regulation, and functions. *Small GTPases*. 2014;5:1, e28003.
76. Porcu G, Parsons AB, Di Giandomenico D, et al. Combined p21-activated kinase and farnesyltransferase inhibitor treatment exhibits enhanced anti-proliferative activity on melanoma, colon and lung cancer cell lines. *Mol Cancer*. 2013;12:88.
77. Orr AW, Hahn C, Blackman BR, Schwartz MA. p21-activated kinase signaling regulates oxidant-dependent NF-kappa B activation by flow. *Circ Res*. 2008;103:671–679.
78. Chiang YT, Jin T. p21-Activated protein kinases and their emerging roles in glucose homeostasis. *Am J Physiol Endocrinol Metab*. 2014;306:E707–E722.
79. Basak C, Pathak SK, Bhattacharyya A, Mandal D, Pathak S, Kundu M. NF-kappaB- and C/EBPbeta-driven interleukin-1beta gene expression and PAK1-mediated caspase-1 activation play essential roles in interleukin-1beta release from Helicobacter pylori lipopolysaccharide-stimulated macrophages. *J Biol Chem*. 2005;280:4279–4288.
80. Williams DS, Arikawa K, Paallysaho T. Cytoskeletal components of the adherens junctions between the photoreceptors and the supportive Muller cells. *J Comp Neurol*. 1990;295:155–164.
81. Carbajal JM, Gratrix ML, Yu CH, Schaeffer RC Jr. ROCK mediates thrombin's endothelial barrier dysfunction. *Am J Physiol Cell Physiol*. 2000;279:C195–C204.
82. Mikelis CM, Simaan M, Ando K, et al. RhoA and ROCK mediate histamine-induced vascular leakage and anaphylactic shock. *Nat Commun*. 2015;6:6725.
83. Aslam M, Schluter KD, Rohrbach S, et al. Hypoxia-reoxygenation-induced endothelial barrier failure: role of RhoA, Rac1 and myosin light chain kinase. *J Physiol*. 2013;591:461–473.
84. Di Lorenzo A, Lin MI, Murata T, et al. eNOS-derived nitric oxide regulates endothelial barrier function through VE-cadherin and Rho GTPases. *J Cell Sci*. 2013;126:5541–5552.
85. Zhang P, Bai H, Fu C, et al. RacGAP1-driven focal adhesion formation promotes melanoma transendothelial migration through mediating adherens junction disassembly. *Biochem Biophys Res Commun*. 2015;459:1–9.
86. Daneshjou N, Sieracki N, van Nieuw Amerongen GP, Schwartz MA, Komarova YA, Malik AB. Rac1 functions as a reversible tension modulator to stabilize VE-cadherin trans-interaction. *J Cell Biol*. 2015;208:23–32.
87. Lui WY, Lee WM, Cheng CY. Sertoli-germ cell adherens junction dynamics in the testis are regulated by RhoB GTPase via the ROCK/LIMK signaling pathway. *Biol Reprod*. 2003;68:2189–2206.
88. Ahmad FJ, Hughey J, Wittmann T, Hyman A, Greaser M, Baas PW. Motor proteins regulate force interactions between microtubules and microfilaments in the axon. *Nat Cell Biol*. 2000;2:276–280.
89. Joshi HC, Chu D, Buxbaum RE, Heidemann SR. Tension and compression in the cytoskeleton of PC 12 neurites. *J Cell Biol*. 1985;101:697–705.
90. Dennerll TJ, Joshi HC, Steel VL, Buxbaum RE, Heidemann SR. Tension and compression in the cytoskeleton of PC-12 neurites. II: quantitative measurements. *J Cell Biol*. 1988;107:665–674.
91. Gorovoy M, Niu J, Bernard O, et al. LIM kinase 1 coordinates microtubule stability and actin polymerization in human endothelial cells. *J Biol Chem*. 2005;280:26533–26542.
92. Prudent R, Vassal-Stermann E, Nguyen CH, et al. Pharmacological inhibition of LIM kinase stabilizes microtubules and inhibits neoplastic growth. *Cancer Res*. 2012;72:4429–4439.
93. Ray S, Fanti JA, Macedo DP, Larsen M. LIM kinase regulation of cytoskeletal dynamics is required for salivary gland branching morphogenesis. *Mol Biol Cell*. 2014;25:2393–2407.
94. Oku Y, Tareyanagi C, Takaya S, et al. Multimodal effects of small molecule ROCK and LIMK inhibitors on mitosis, and their implication as anti-leukemia agents. *PLoS One*. 2014;9:e92402.
95. Acevedo K, Li R, Soo P, et al. The phosphorylation of p25/TPPP by LIM kinase 1 inhibits its ability to assemble microtubules. *Exp Cell Res*. 2007;313:4091–4106.
96. Tojima T, Takahashi M, Ito E. Dual regulation of LIM kinase 1 expression by cyclic AMP and calcium determines cofilin phosphorylation states during neuritogenesis in NG108-15 cells. *Brain Res*. 2003;985:43–55.
97. Takemura M, Mishima T, Wang Y, et al. Ca2+/calmodulin-dependent protein kinase IV-mediated LIM kinase activation is critical for calcium signal-induced neurite outgrowth. *J Biol Chem*. 2009;284:28554–28562.
98. Wang Y, Shibasaki F, Mizuno K. Calcium signal-induced cofilin dephosphorylation is mediated by Slingshot via calcineurin. *J Biol Chem*. 2005;280:12683–12689.
99. Bravo-Cordero JJ, Magalhaes MAO, Eddy RJ, Hodgson L, Condeelis J. Functions of cofilin in cell locomotion and invasion. *Nat Rev Mol Cell Biol*. 2013;14:405–415.

Investigative Ophthalmology & Visual Science